Inertial Confinement Fusion Using the OMEGA Laser System

P. B. Radha, R. Betti, T. R. Boehly, J. A. Delettrez, D. H. Edgell, V. N. Goncharov, I. V. Igumenshchev, J. P. Knauer, J. A. Marozas, F. J. Marshall, R. L. McCrory, D. D. Meyerhofer, S. P. Regan, T. C. Sangster, W. Seka, S. Skupsky, A. A. Solodov, C. Stoeckl, W. Theobald, J. A. Frenje, D. T. Casey, C. K. Li, and R. D. Petrasso

***Abstract*—The OMEGA laser system is being used to investigate several approaches to inertial confinement fusion: the traditional central-hot-spot (CHS) ignition, fast ignition (FI), and shock ignition (SI). To achieve ignition, CHS requires the highly uniform compression of a solid deuterium–tritium (DT)-layered target on a low adiabat (defined as the ratio of the pressure to the Fermi-degenerate pressure) and with an implosion velocity $V_{\rm imp} \geq 3.5 \times 10^7$ cm/s. A laser pulse shape with triple pickets is used to produce this low adiabat by optimally timing multiple shocks launched by the pickets and the main laser. Cryogenic targets that imploded optimally with such pulses have demonstrated near-design compression with an areal density $\rho R \sim 290$ mg/cm^2 at $V_{\rm imp} = 3.1 \times 10^7$ cm/s. These are, by far, the highest DT areal densities demonstrated in the laboratory. SI experiments, where a shock is launched by a picket at the end of the laser pulse into the compressing capsule, have been performed on low-adiabat warm plastic targets. Both yield and areal density improve significantly when a spike is used at the end of the laser pulse, indicating that the energy from the shock is coupled into the compressing target. Integrated FI experiments have begun on the OMEGA/OMEGA EP laser system.**

***Index Terms*—Confinement, direct drive, fusion, inertial.**

I. Introduction

FUSION energy is arguably the holy grail of energy research. At the University of Rochester's Laboratory for Laser Energetics, a few of the many approaches to inertial confinement fusion are being studied [1]–[3]. In these approaches, a layer of cryogenic deuterium–tritium (DT) is accelerated like a rocket by the laser-driven ablation of the outer-shell material. In the hot-spot approach, the PdV work by the converging shell raises the temperature of the hot spot to ~10 keV and the areal density to ~300 mg/cm^2. Typical laser pulse shapes and targets that can achieve these conditions are shown schematically in Fig. 1(a). Under these hot-spot conditions, the 3.5-MeV alpha particles from the DT fusion reactions are stopped in the target, causing a propagating burn [Fig. 1(b)]. Obtaining these conditions requires a high level of uniformity in the laser drive and targets. Nonuniformities are seeded by laser-beam variations, single-beam speckle, and target-surface nonuniformities [4]. These seeds are amplified by Rayleigh–Taylor (RT) [5], [6] instability at the ablation surface during acceleration and feed through and grow on the inside of the shell when the shell decelerates. Nonuniformity growth reduces the hot-spot radius and can cool it, preventing burn propagation [7].

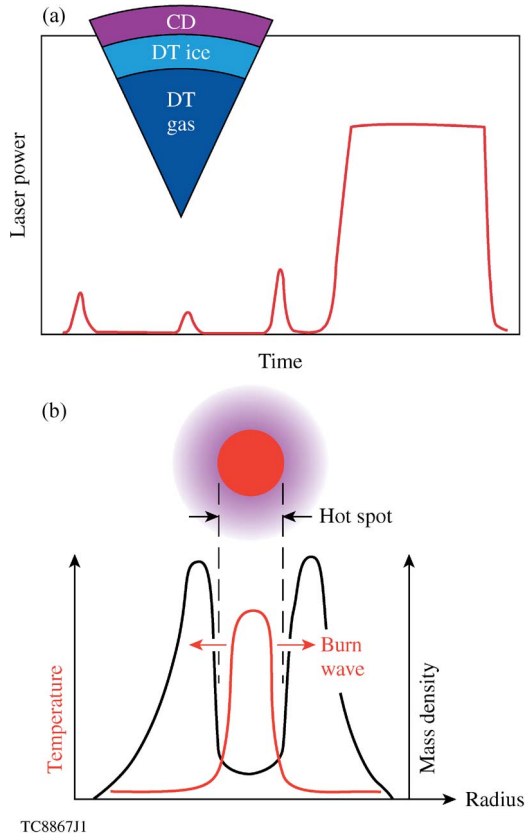

Fig. 1. (a) Typical target comprising a layer of deuterated plastic (CD) enclosing a cryogenic layer of DT and pulse shape for hot-spot ignition. (b) Density and temperature profiles in the compressed core at the onset of ignition.

Manuscript received September 16, 2010; revised December 14, 2010; accepted January 20, 2011. Date of publication March 9, 2011; date of current version April 13, 2011. This work was supported by the U.S. Department of Energy Office of Inertial Confinement Fusion under Cooperative Agreement DE-FC52-08NA28302, by the University of Rochester, and by the New York State Energy Research and Development Authority.

P. B. Radha, T. R. Boehly, J. A. Delettrez, D. H. Edgell, V. N. Goncharov, I. V. Igumenshchev, J. P. Knauer, J. A. Marozas, F. J. Marshall, S. P. Regan, T. C. Sangster, W. Seka, S. Skupsky, A. A. Solodov, C. Stoeckl, and W. Theobald are with the Laboratory for Laser Energetics, University of Rochester, Rochester, NY 14623 USA (e-mail: rbah@lle.rochester.edu).

R. Betti, R. L. McCrory, and D. D. Meyerhofer are with the Laboratory for Laser Energetics and the Department of Mechanical Engineering and Physics, University of Rochester, Rochester, NY 14623 USA.

J. A. Frenje, D. T. Casey, C. K. Li, and R. D. Petrasso are with the Plasma Science and Fusion Center, Massachusetts Institute of Technology, Cambridge, MA 02139 USA.

Color versions of one or more of the figures in this paper are available online at http://ieeexplore.ieee.org.

Digital Object Identifier 10.1109/TPS.2011.2109949

0093-3813/$26.00 © 2011 IEEE

The gain G (defined as the ratio of the thermonuclear energy produced from the DT fusion reactions to the laser energy) depends on the implosion velocity $V_{\rm imp}$ (the velocity of the imploding shell at peak kinetic energy) and the burn-up fraction θ and is given by [8]

$$G = \frac{E_{\rm fus}}{E_{\rm laser}} \sim V_{\rm imp}^{-1.25}\theta(\rho R) \sim \frac{V_{\rm imp}^{-1.25}}{1+7/\rho R} \tag{1}$$

where $\theta(\rho R) = 1/(1+7/\rho R)$ is a measure of the confinement time of the plasma that depends on the areal density $\rho R = \int \rho dr$. For typical ignition targets, it is required that the areal density of the compressed shell be greater than $\sim$1100 mg/cm^2 to provide significant gain.

The maximum areal density in an implosion has been shown to depend primarily on the adiabat on the inside of the shell $\alpha_{\rm inn}$, defined by the ratio of the pressure to the Fermi-degenerate pressure at peak density, and the laser energy E_L [9] and is given by

$$\rho R_{\max}({\rm mg/cm^2}) = \frac{2.6\times 10^2 E_{\rm L}^{1/3}({\rm kJ})}{\alpha_{\rm inn}^{0.6}}. \tag{2}$$

As (2) shows, areal density depends primarily on $\alpha_{\rm inn}$. Achieving the appropriate adiabat requires the optimal timing of shocks launched at different times in the laser pulse. For example, for the pulse shape shown in Fig. 1(a), it is critical that the shocks launched by each of the pickets and the main pulse coalesce very close to the inner portion of the shell at or shortly after they break out of the shell. If the catch-up is too early or too late, the adiabat $\alpha_{\rm inn}$ will be higher, leading to a smaller areal density.

Equation (1) assumes that ignition has taken place and indicates that a higher gain can be obtained with a lower implosion velocity since a larger mass needs to be assembled to obtain a lower implosion velocity for the same laser energy. A lower implosion velocity, however, raises the minimum energy required for hot-spot ignition. The minimum energy for ignition scales as

$$E_{\min}({\rm kJ}) = 50.8\alpha_{\rm inn}^{1.88}(V_{\rm imp}/3\times 10^7\ {\rm cm/s})^{-5.89} \times (P/100\ {\rm Mbar})^{-0.77} \tag{3}$$

where P is the pressure on the outside of the shell when it reaches the implosion velocity [10]. Higher velocity implosions are required to ignite at laser energies achievable by current laser technologies. For example, simulations indicate that hot-spot ignition on the 1.5-MJ National Ignition Facility (NIF) [11], [12] requires $\alpha_{\rm inn} \sim 2$ to 4 and $V_{\rm imp} \geq 3.5\times 10^7$ cm/s [13].

The imploding shell gains kinetic energy primarily through collisional absorption (inverse Bremsstrahlung laser energy absorption) in the corona of the target [14] for the methods described in this paper. Deviations on the order of $\sim$10% from the inverse Bremsstrahlung total energy absorption have been observed recently [15] and attributed to nonlinear plasma processes such as cross-beam energy transfer induced by stimulated Brillouin scattering [16]. Recent models [17] developed to simulate this process account for the observed scattered light

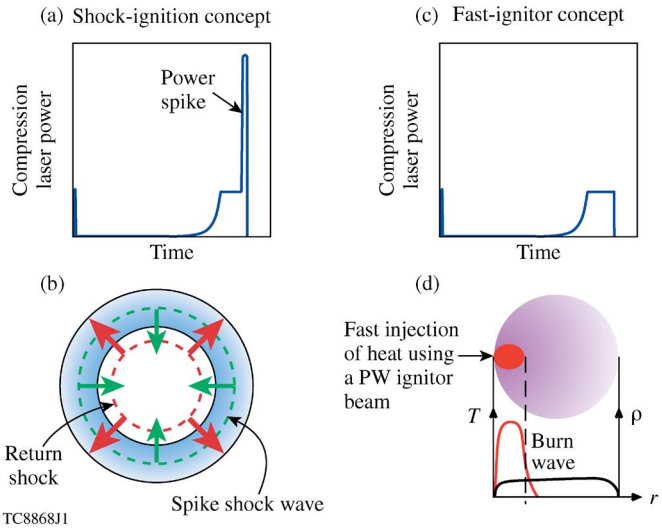

Fig. 2. (a) Typical pulse shape for SI. (b) Schematic showing the reflected shock from the compression laser and the converging shock caused by the spike at the end of the laser pulse. (c) Typical pulse shape for FI. (d) Schematic showing the compressed core ignited by the deposition of energy from electrons generated using a petawatt laser.

and also the time of neutron production, sensitive observables of the laser drive. This has led to greater confidence in the modeling of the shell implosion velocity.

Hydrodynamically, higher velocity implosions are less stable than lower velocity implosions. The number of e-foldings attributable to RT growth N_e for the most dangerous mode $k\Delta_{\rm if} \approx 1$, where k is the wavenumber and $\Delta_{\rm if}$ is the in-flight shell thickness, is used to characterize stability. This, in turn, can be written in terms of the in-flight aspect ratio (IFAR), the ratio of the average shell radius R to shell thickness given by [18]

$$IFAR = \frac{R}{\Delta_{\rm if}} = \frac{60(V_{\rm imp}/3\times 10^7\ {\rm cm/s})^2}{\langle\alpha\rangle^{0.6} I_{15}^{0.27}} \tag{4}$$

where $\langle\alpha\rangle$ is the density-averaged adiabat in the shell and I_{15} is the on-target intensity in units of 10^{15} W/cm^2. The number of RT e-foldings scales as $N_e(k\Delta_{\rm if}=1) \sim \sqrt{IFAR}$ [13]. Too high an IFAR reduces target performance by degrading compression and reducing the yield from fusion reactions. Too low an IFAR raises the minimum energy required for ignition through its dependence on implosion velocity.

Both shock ignition (SI) [2] and fast ignition (FI) [3] schemes ease the energy constraints on the compression laser by making it possible for ignition to occur at lower implosion velocities or lower values of IFAR. In the SI concept, a spike at the end of the laser pulse launches a shock to ignite the compressed fuel [Fig. 2(a)]. It is critical to time this shock such that it meets the reflected shock from the center just inside the shell [Fig. 2(b)]. The resultant converging shock raises the hot-spot temperature and density and initiates ignition. SI requires a high degree of uniformity to assemble fuel and effectively heat the hot spot. In FI, the shell is heated externally to initiate burn (Fig. 2). In one realization of FI, the external heating is provided by stopping the approximately megaelectronvolt electrons produced by a petawatt laser. A gold cone is used to keep the plasma away

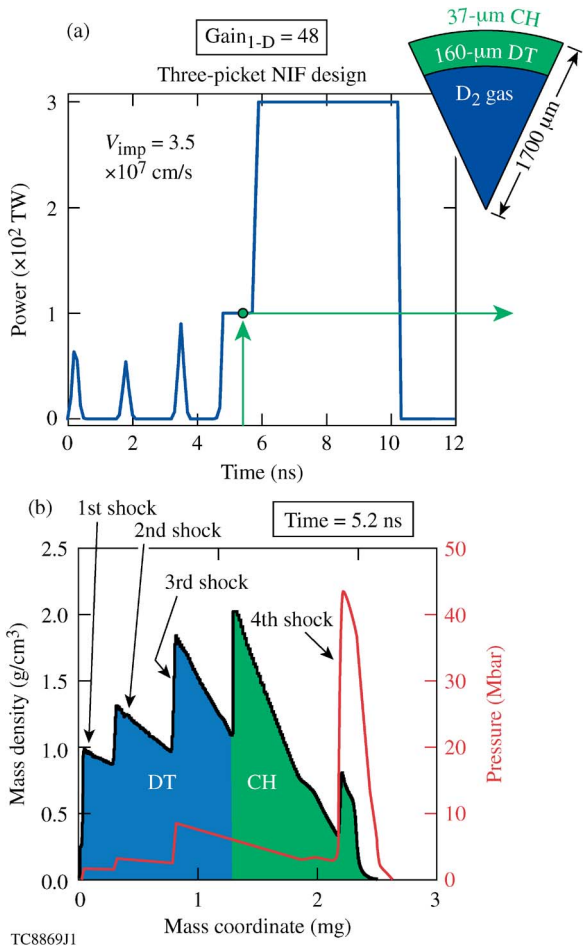

Fig. 3. (a) Three-picket ignition design for the NIF. (b) Location of shocks in the three-picket design. (Left axis) Mass density versus mass coordinate. (Right axis) Pressure versus mass coordinate.

from the region on which the petawatt laser is focused [19]. A different way to achieve ignition using petawatt lasers is to channel a hole through the plasma surrounding the high-density shell and directly heat the fuel [3]. The uniformity requirement on the compression laser is relaxed for FI because the hot spot does not have to initiate burn. Both FI and SI require the assembly of high-areal-density fuel and therefore depend crucially on achieving the optimal shock timing.

II. Hot-Spot Ignition

The ignition design for the NIF (Fig. 3) comprises a 37-μm plastic (CH) shell containing a 160-μm DT layer with a nominal radius of 1700 μm [20]. The pulse shape used to drive this target is also shown in Fig. 3, corresponding to a peak on-target intensity of $\sim 8.5 \times 10^{14}$ W/cm^2 at the initial target radius or an actual intensity, which is about a factor of approximately two higher at the critical region at the end of the laser pulse because of its convergence. This target has a gain of 48 in 1-D simulations. The sequence of shocks launched by the pickets and the main pulse is shown in Fig. 3(b). It is critical to time the shocks launched by each picket and the main pulse such that they coalesce shortly after they break out of the shell. If they catch up with each other in the shell or well after they

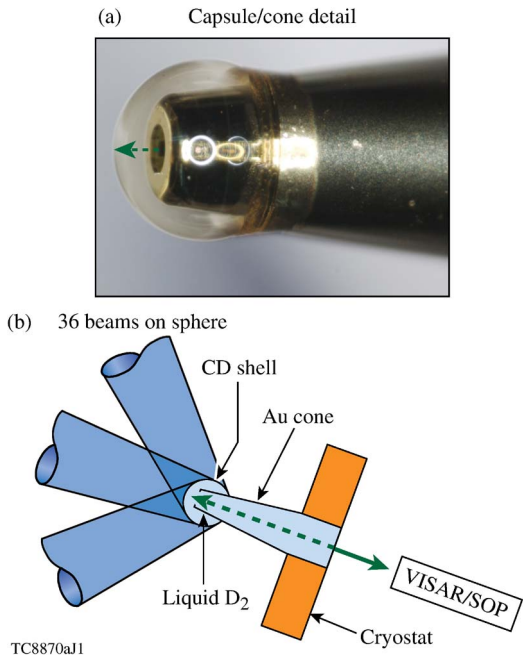

Fig. 4. (a) Cone-in-shell target used for measuring shock velocities. (b) Schematic of the setup used to measure shock velocities. (a) Capsule/cone detail. (b) 36 beams on sphere.

break out of the shell, they raise $\alpha_{\rm inn}$ and reduce areal density and, therefore, the confinement time.

The OMEGA laser [21] is used to study the various aspects of directly driven fusion approaches discussed in Section I. Shock velocities are measured on the OMEGA laser using cone-in-shell targets [Fig. 4(a)] [22]. These targets comprise a gold cone inserted into a spherical CH shell containing liquid deuterium. Fig. 4(b) shows a schematic of the experiment, where 36 laser beams directly irradiate the hemisphere of the shell. The velocity interferometer system for any reflector (VISAR) [23] is used to measure temporally resolved optical fringes; the slope of the fringes provides the shock velocity, and an abrupt shift in the fringes indicates shock coalescence. A streaked optical pyrometer (SOP) [24] is used to measure the self-emission caused by shocks. Two different laser pulse shapes in shock-timing experiments [22] are shown in Fig. 5(a) and (c). Simulations of shock velocities and measured values are shown in Fig. 5(b) and (d). Simulations are performed using the 1-D hydrodynamic code *LILAC* [25] with inverse Bremsstrahlung laser deposition and a flux-limited ($f = 0.06$, sharp cutoff) heat conduction model. For both cases, the shock velocities agree well with the simulated velocities. The measured shock coalescence times agree with simulations. In addition, the catch-up of the main shock with the earlier shocks from the pickets is also modeled well [Fig. 5(d)]; the VISAR signal blanks when the main shock overtakes the picket shocks and the time of this blanking agrees well with the main shock catch-up in simulations. The SOP signal confirms the catch-up of the main shock. The remaining discrepancies in shock velocities and catch-up times have a marginal effect on ignition and are attributed to the cryogenic target not being placed at the target chamber center. Experiments and modeling are ongoing to measure the target offset on each shot and include them in

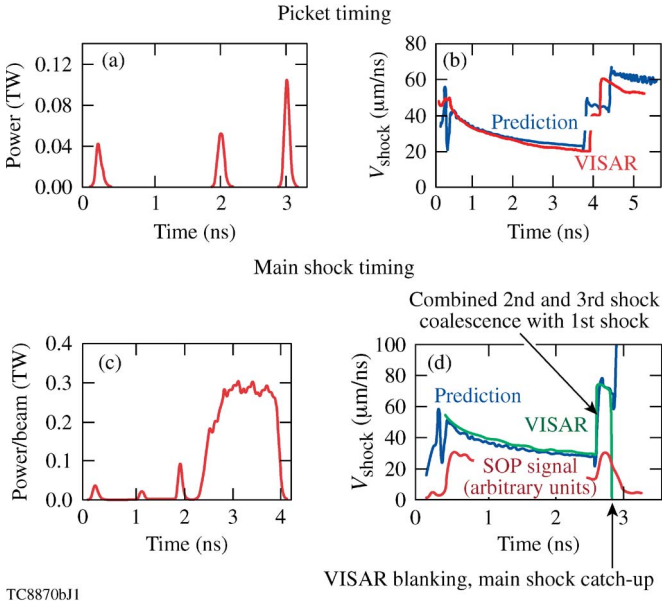

Fig. 5. Typical comparison of simulated and observed shock velocities. (a) Pulse shapes with three pickets. (b) (Blue) Simulated and measured shock velocities using (red) VISAR. (c) Triple-picket pulse shape including the main pulse. (d) (Blue) Simulated and (red) measured shock velocities. The (green) signal from the SOP shows the coalescence of the first shock with the second and third shocks.

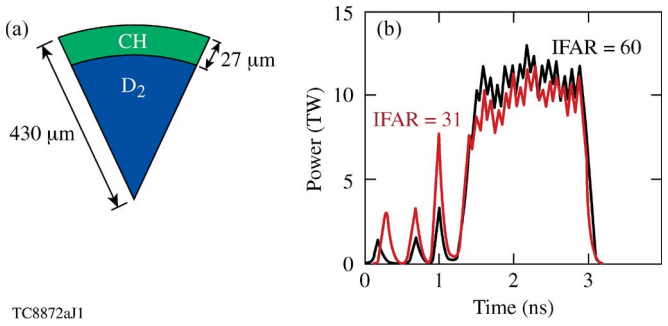

Fig. 6. (a) Schematic of target used to demonstrate the optimal value of IFAR. (b) Triple-picket pulse shapes used to obtain different IFARs.

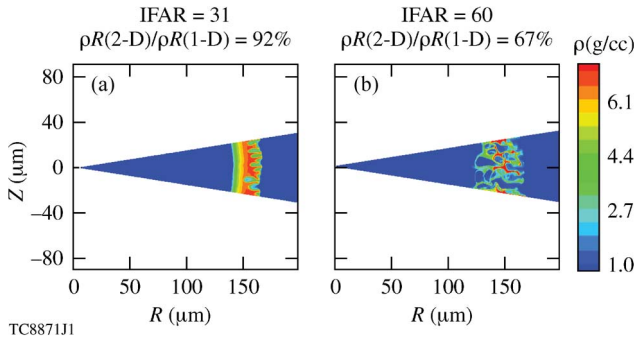

Fig. 7. Density contour at the end of the acceleration phase for (a) $IFAR \sim 31$ targets and (b) $IFAR \sim 60$ targets.

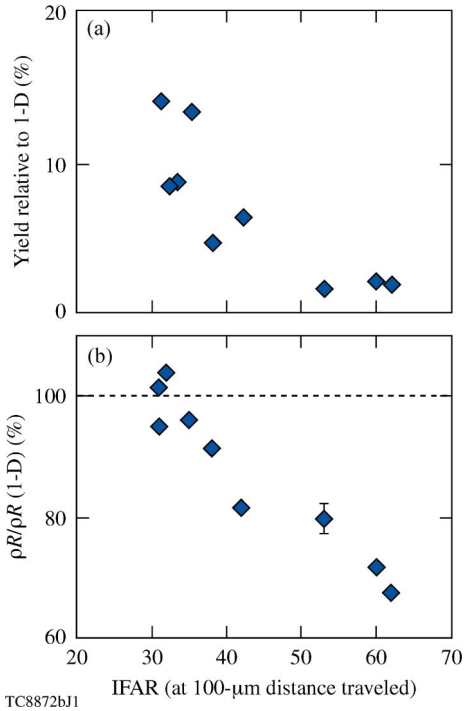

Fig. 8. (a) Ratio (in percent) of the measured and simulated yields versus calculated IFAR. (b) Ratio (in percent) of the measured and simulated areal densities versus calculated IFAR.

the simulations. These independent shock-timing experiments provide confidence that the predicted compression in implosion experiments will be achieved.

Implosion experiments to study the physics of the hot-spot approach are being conducted on the OMEGA laser using varying targets and pulse shapes [20], [26]. To identify the optimal range of IFAR, implosions have been conducted on 9-atm deuterium-filled 27-μm-thick warm plastic (CH) shells with a nominal diameter of 860 μm [Fig. 6(a)] [26]. These targets are directly irradiated with pulse shapes that have three pickets, followed by a rise to constant intensity of $\sim 4.5 \times 10^{14}$ W/cm^2. The IFAR in these implosions is varied by changing the picket energies and timing among them [Fig. 6(b)] such that $\langle \alpha \rangle$ varies systematically. Implosion velocities are between 2.6×10^7 and 2.8×10^7 cm/s. Fig. 7 shows the density contours at the end of the acceleration phase for the implosions with $IFAR \sim 31$ and $IFAR \sim 60$, simulated using the 2-D axisymmetric hydrodynamic code *DRACO* [4]. The high IFARs result in considerable distortion of the shell and reduce compression. Only 72% of the peak 1-D compression is achieved in the $IFAR \sim 60$ implosions, compared to nearly 100% of 1-D compression for the $IFAR \sim 31$ implosion. Target performance is quantified by comparison with 1-D simulations using the radiation hydrodynamic code *LILAC*. As Fig. 8(a) shows, the ratio of the measured to the simulated 1-D neutron yield decreases with increasing IFAR. Areal densities are measured through the energy loss of the secondary protons [27]. The ratio of the measured areal density to the 1-D-simulated value [Fig. 8(b)] also degrades with increasing IFAR. These measurements indicate that IFAR #40 is required to achieve adequate compression. The ignition design described previously has $IFAR \sim 40$.

Cryogenic-DT-layer implosions have been performed with triple-picket pulse shapes [20]. The target comprises an $\sim$10-μm CH shell with an outer diameter of 860 μm, containing an $\sim$65-μm-thick frozen DT layer [Fig. 9(a)]. It is directly

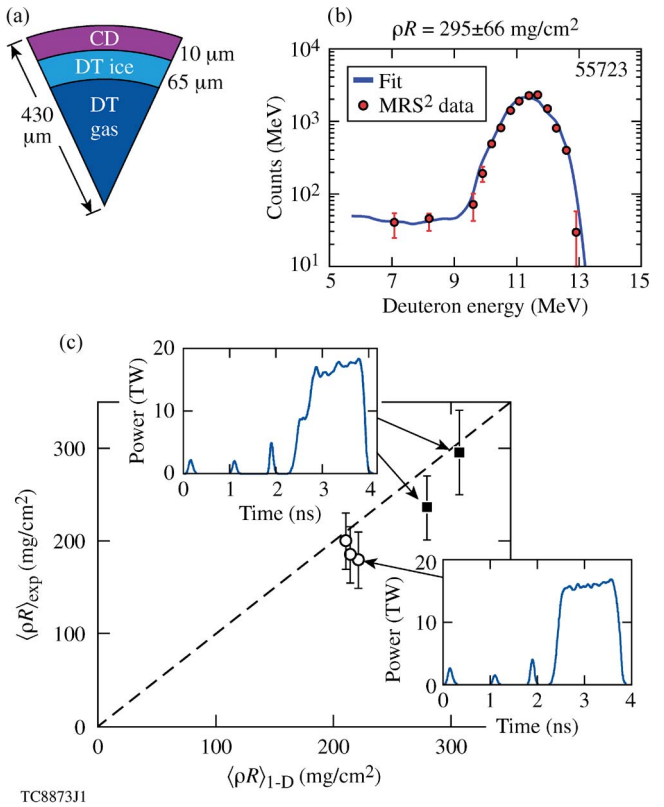

Fig. 9. (a) Schematic of target used to demonstrate high compression. (b) Measured counts/megaelectronvolt versus deuteron energy from (red points) the MRS and (solid line) the fit to MRS data using an ice-block model. The inferred areal density is $\rho R = 295 \pm 66$ mg/cm^2. (c) Measured areal density versus the simulated areal densities for different pulse shapes in cryogenic-DT implosions. The insets show the laser pulse shapes used to drive the target in (a).

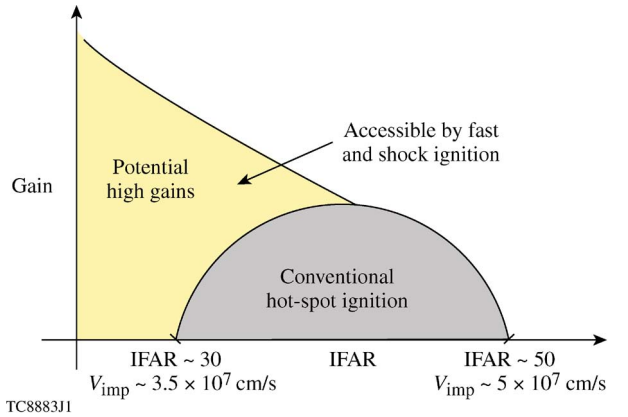

Fig. 10. Schematic showing the various ignition approaches in IFAR space.

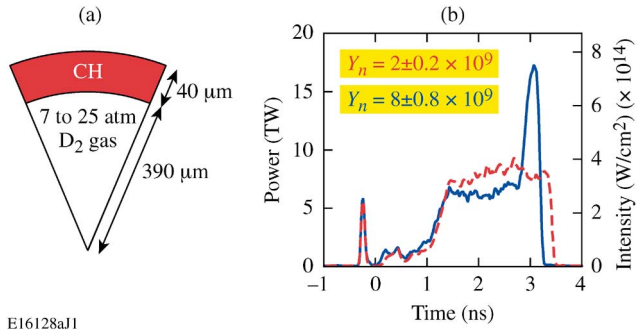

Fig. 11. (a) Schematic of target used to demonstrate SI. (b) Pulse shapes used to test the performance of SI pulse shapes (solid line) with and (dashed line) without a picket.

driven by two different laser pulse shapes: a triple-picket series followed by a sharp rise to constant intensity and a triple-picket series followed by a constant intensity pulse with a step [insets of Fig. 9(c)]. These implosions have $IFAR \sim 35$ with $V_{\rm imp} \sim 3.1 \times 10^7$ cm/s. The areal densities in these implosions are inferred from the spectrum of down-scattered neutrons measured using a magnetic recoil spectrometer (MRS) [28]. The ratio of the number of down-scattered neutrons to the primary DT neutron yield is proportional to areal density. Fig. 9(b) shows the measured deuteron spectrum (points) and the fit to the measurements using an ice-block model (solid line). Down-scattered and primary neutrons, incident on a deuterated polymer (CD) foil, scatter deuterons whose spectrum is measured [28]. Using the well-known elastic scattering cross section of neutrons off deuterons, the measured spectrum is fitted using an incident neutron spectrum. An ice-block model with ρR as the parameter is used to calculate the fitted-neutron spectrum. The emergent neutron spectrum from the compressed capsule has a marginal dependence on details of the density profile and depends primarily on the areal density, justifying the use of an ice-block model. This fit provides an areal density $\rho R = 295 \pm 66$ mg/cm^2, which is very close to the 1-D values of 300 mg/cm^2. Fig. 9(c) shows the measured areal densities versus the simulated values for a series of implosions irradiated with both the square and the step main pulses. High values of areal densities can be repeatedly obtained across different shots, indicating the reproducibility of these measurements. These results indicate that high compression of DT—an important requirement for all the three fusion approaches—is achievable. Higher ignition-relevant values of $V_{\rm imp}$ can be achieved by using thinner ~55-μm-thick DT shells. These will be studied in the near future.

III. SI

The region of IFAR space, where ignition can be achieved by these approaches, is shown in Fig. 10. At low values of IFAR, both SI and FI show promise of large gains because of the low implosion velocity in both these schemes. Encouraging results for SI have been obtained on OMEGA using warm CH shells [29]. The target has a 40-μm-thick CH shell, with a nominal diameter of 860 μm, filled with D_2 gas at different pressures [Fig. 11(a)]. The pulse shapes used to drive this target are shown in Fig. 11(b). An initial picket is used to set the adiabat profile in the shell: $\alpha_{\rm inn} \sim 1.5$ for these implosions. By design, the no-spike pulse shape has a slightly higher peak power; the energy difference is used to form the spike. Different timings of the spike have been used to study the target performance in the implosion experiments. The measured neutron yield increases significantly when the spike is added toward the end of the laser pulse. The optimally timed spike is shown in Fig. 11(b); the neutron yield increases by nearly a factor of four when the spike shock is used. This enhancement in yield is larger than

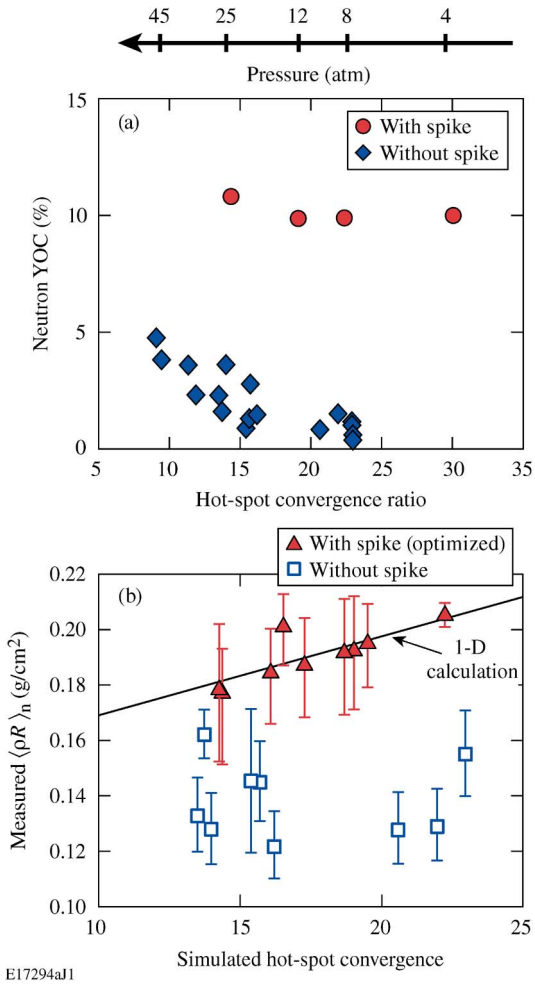

Fig. 12. (a) Ratio of the measured to the simulated neutron yield (in percent) versus the hot-spot convergence ratio for (circles) an SI pulse compared to (diamonds) a standard pulse. (b) Measured areal density versus hot-spot convergence ratio [(triangles) with SI spike; (squares) without SI spike]. The solid line indicates the simulated areal densities as a function of hot-spot convergence ratio.

the simulated one; simulations indicate that the use of the spike at the end of the laser pulse should enhance yield by up to 30%, depending on the spike timing. These results indicate that it is possible to raise the ion temperature in the hot core using an optimally launched shock toward the end of the laser pulse.

Fig. 12 shows a summary of results from a series of shots where the convergence ratio (defined as the ratio of the initial to the final radius of the hot spot) is varied. Differing convergence ratios are obtained by changing the pressure of the D_2-gas fill. When the spike is not used, the ratio of the measured yield to the 1-D yield decreases with the convergence ratio [Fig. 12(a)]. Since these implosions have very low IFAR ($\sim$12), their performance is not significantly influenced by RT growth during acceleration; instead, the RT growth during deceleration compromises performance. Nonuniformity growth reduces the clean hot-spot volume, reducing yield. Significantly better performance, as measured by this ratio, is obtained when the spike is used. This is likely due to the reduced time available for deceleration-phase RT growth caused by the impulsive acceleration of the shell by the reconverging shock. Similarly, higher ratios of the measured to simulated 1-D areal densities

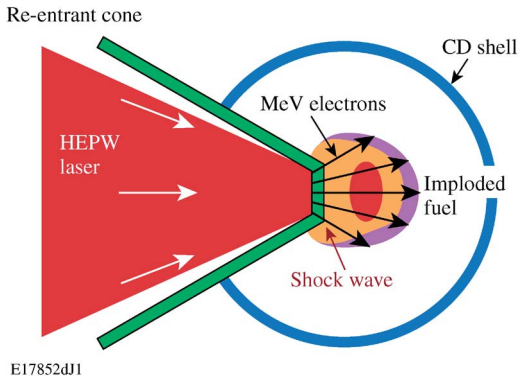

Fig. 13. Schematic of a gold cone-in-shell target showing the imploded core and the energetic electrons launched by the petawatt laser.

are obtained when the spike is used [Fig. 12(b)]. The measured areal densities are in good agreement with the 1-D-simulated areal densities when the spike is used. Since the areal-density measurement uses secondary proton energy loss, it can be measured only when fusion reactions occur. The measured improvement in areal density with a spike is primarily due to the higher neutron yield and, consequently, the improved sampling of the areal-density history.

IV. FI

The FI approach being investigated on OMEGA uses cone-in-shell targets (Fig. 13) [30]. The purpose of the gold cone is to keep the coronal plasma away from the region around the target where the petawatt beam is focused. This allows the petawatt beam to be deposited in a region close to the high-density shell, which, in turn, makes it possible for energetic electrons (approximately megaelectronvolts), caused by laser–plasma instabilities, to reach the shell and deposit their energy. The coupling efficiency of the laser depends on a number of factors, including the conversion of laser energy to electrons, the energy spectrum of the electrons, the collimation of electron transport, the distance from the cone tip to the dense shell where the electrons deposit their energy, and the shape of the cone. Integrated experiments using the OMEGA/OMEGA EP [31] laser system have begun to address these issues. The target has a nominal 860-μm diameter with a 40-μm CD shell and a reentrant gold cone. Two-dimensional simulations that use the hydrodynamic code *DRACO* and the particle-in-cell beam that has an energy of $\sim$1 kJ with a 10-ps duration at a code *LSP* [32] have been performed [33]. *DRACO* includes the compression physics, and *LSP* is used to transport the electrons from where they are produced to the dense shell where they deposit their energy. The target is directly driven with an OMEGA laser pulse shape similar to the low-adiabat picket pulse shape in Fig. 11(b) (dashed lines). The OMEGA EP beam has an energy of $\sim$1 kJ with a 10-ps duration at a wavelength of 1053 nm and an intensity of $\sim 1 \times 10^{19}$ W/cm^2. The petawatt beam is focused onto a spot of $\sim$40-μm radius. The relative timing of the petawatt beam with the compression laser is varied. The density contours from simulation are shown in Fig. 14. The presence of the gold cone does not disrupt compression; high areal densities are achieved in this implosion. The integrated

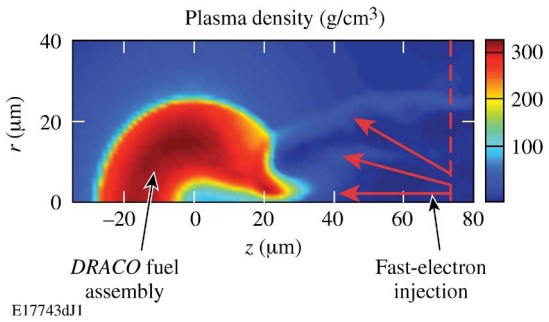

Fig. 14. Density contours from a 2-D simulation including a gold cone. A fast-electron beam is transported into the imploded core using the code *LSP*.

simulations indicate that 2.3×10^7 neutrons (corresponding to $\sim$5% of the 1-D yield) should be additionally produced in the implosions, where the petawatt beam is optimally timed with respect to the compression pulse shape. This corresponds to a coupling efficiency of $\sim$10%. These simulations indicate that the higher coupling efficiency of the electrons is due to the collimation by the self-generated magnetic fields. Preliminary results from these experiments indicate an improved observed yield; $\sim 2.5 \times 10^7$ additional neutrons, corresponding to a four-fold increase, are observed [34]. Higher short-pulse energies, advanced targets including those with lower Z cones, and the extent of electron collimation using materials with different electron resistivities will be explored in the future to optimize the laser energy coupled into the plasma.

V. Conclusion

The OMEGA/OMEGA EP laser system is being used to study a variety of approaches to direct-drive inertial confinement fusion: the traditional central-hot-spot approach, FI, and SI. A laser pulse shape with three pickets produces the low adiabat required for the hot-spot approach. The timing of multiple shocks launched by the pickets and the main laser pulse is optimized in experiments using a cone-in-shell geometry. Cryogenic targets imploded with optimally timed low-adiabat triple-picket pulses have demonstrated near-1-D compression with an areal density $\rho R \sim 290$ mg/cm^2 at $V_{\rm imp} = 3.1 \times 10^7$ cm/s. These are, by far, the highest DT areal densities demonstrated in the laboratory. Using thinner shells will increase implosion velocities and achieve ignition scaling. SI experiments, where a shock is launched by a picket at the end of the laser pulse into the compressing capsule, have been performed on low-adiabat warm plastic targets. Both yield and areal density improve significantly when a spike is used at the end of the laser pulse, indicating that the energy from the shock is coupled into the compressing target. Integrated FI experiments have begun on the OMEGA/OMEGA EP laser system. A 10-ps 1-kJ OMEGA EP beam is pointed into the tip of a gold cone inserted into a thick-plastic converging and compressing shell. Two-dimensional simulations that couple the transport of energetic electrons using the code *LSP* with the hydrodynamic evolution using the code *DRACO* indicate that neutron yields would increase by $\sim 2.3 \times 10^7$ neutrons for a 10% coupling efficiency of hot electrons.

Acknowledgment

The support of the Department of Energy (DOE) does not constitute an endorsement by DOE of the views expressed in this paper.

References

[1] J. Nuckolls, L. Wood, A. Thiessen, and G. Zimmerman, "Laser compression of matter to super-high densities: Thermonuclear (CTR) applications," *Nature*, vol. 239, pp. 139–142, Sep. 1972.

[2] R. Betti, C. D. Zhou, K. S. Anderson, L. J. Perkins, W. Theobald, and A. A. Solodov, "Shock ignition of thermonuclear fuel with high areal density," *Phys. Rev. Lett.*, vol. 98, no. 15, p. 155 001, Apr. 2007.

[3] M. Tabak, J. Hammer, M. E. Glinsky, W. L. Kruer, S. C. Wilks, J. Woodworth, E. M. Campbell, M. D. Perry, and R. J. Mason, "Ignition and high gain with ultrapowerful lasers," *Phys. Plasmas*, vol. 1, no. 5, pp. 1626–1634, May 1994.

[4] P. B. Radha, V. N. Goncharov, T. J. B. Collins, J. A. Delettrez, Y. Elbaz, V. Y. Glebov, R. L. Keck, D. E. Keller, J. P. Knauer, J. A. Marozas, F. J. Marshall, P. W. McKenty, D. D. Meyerhofer, S. P. Regan, T. C. Sangster, D. Shvarts, S. Skupsky, Y. Srebro, R. P. J. Town, and C. Stoeckl, "Two-dimensional simulations of plastic-shell, direct-drive implosions on OMEGA," *Phys. Plasmas*, vol. 12, no. 3, pp. 032 702-1–032 702-18, Mar. 2005.

[5] L. Rayleigh, "Investigation of the character of the equilibrium of an incompressible heavy fluid of variable density," in *Proc. London Math. Soc.*, 1883, vol. XIV, pp. 170–177.

[6] G. Taylor, "The instability of liquid surfaces when accelerated in a direction perpendicular to their planes. I," *Proc. R. Soc. Lond. Ser. A*, vol. 201, no. 1065, pp. 192–196, Mar. 1950.

[7] R. Kishony and D. Shvarts, "Ignition condition and gain prediction for perturbed inertial confinement fusion targets," *Phys. Plasmas*, vol. 8, no. 11, pp. 4925–4936, Nov. 2001.

[8] G. S. Fraley, E. J. Linnebur, R. J. Mason, and R. L. Morse, "Thermonuclear burn characteristics of compressed deuterium–tritium microspheres," *Phys. Fluids*, vol. 17, no. 2, pp. 474–489, Feb. 1974.

[9] R. Betti and C. Zhou, "High-density and high- ρR fuel assembly for fast-ignition inertial confinement fusion," *Phys. Plasmas*, vol. 12, no. 11, pp. 110 702-1–110 702-4, Nov. 2005.

[10] M. C. Herrmann, M. Tabak, and J. D. Lindl, "A generalized scaling law for the ignition energy of inertial confinement fusion capsules," *Nucl. Fusion*, vol. 41, no. 1, pp. 99–111, Jan. 2001.

[11] E. I. Moses, "Ignition on the National Ignition Facility," *J. Phys., Conf. Ser.*, vol. 112, no. 1, p. 012 003, 2008.

[12] S. H. Glenzer, B. J. MacGowan, P. Michel, N. B. Meezan, L. J. Suter, S. N. Dixit, J. L. Kline, G. A. Kyrala, D. K. Bradley, D. A. Callahan, E. L. Dewald, L. Divol, E. Dzenitis, M. J. Edwards, A. V. Hamza, C. A. Haynam, D. E. Hinkel, D. H. Kalantar, J. D. Kilkenny, O. L. Landen, J. D. Lindl, S. LePape, J. D. Moody, A. Nikroo, T. Parham, M. B. Schneider, R. P. J. Town, P. Wegner, K. Widmann, P. Whitman, B. K. F. Young, B. Van Wonterghem, L. J. Atherton, and E. I. Moses, "Symmetric inertial confinement fusion implosions at ultra-high laser energies," *Science*, vol. 327, no. 5970, pp. 1228–1231, Mar. 2010.

[13] C. D. Zhou and R. Betti, "Hydrodynamic relations for direct-drive fast-ignition and conventional inertial confinement fusion implosions," *Phys. Plasmas*, vol. 14, no. 7, pp. 072 703-1–072 703-12, Jul. 2007.

[14] P. Mora, "Theoretical model of absorption of laser light by a plasma," *Phys. Fluids*, vol. 25, no. 6, pp. 1051–1056, Jun. 1982.

[15] D. H. Edgell, W. Seka, J. A. Delettrez, R. S. Craxton, V. N. Goncharov, I. V. Igumenshchev, J. F. Myatt, A. V. Maximov, R. W. Short, T. C. Sangster, and R. E. Bahr, "Cross-beam energy transport in direct-drive-implosion experiments," *Bull. Amer. Phys. Soc.*, vol. 54, p. 145, 2009.

[16] W. L. Kruer, "The physics of laser–plasma interactions," in *Frontiers in Physics*, D. Pines, Ed. Redwood City, CA: Addison-Wesley, 1988, ch. 4, pp. 37–43.

[17] I. V. Igumenshchev, D. H. Edgell, V. N. Goncharov, J. A. Delettrez, A. V. Maximov, J. F. Myatt, W. Seka, A. Shvydky, S. Skupsky, and C. Stoeckl, "Crossed-beam energy transfer in implosion experiments on OMEGA," *Phys. Plasmas*, vol. 17, no. 12, pp. 122 708-1–122 708-5, Dec. 2010.

[18] J. D. Lindl, *Inertial Confinement Fusion: The Quest for Ignition and Energy Gain Using Indirect Drive*. New York: Springer-Verlag, 1998.

[19] R. Kodama, H. Shiraga, K. Shigemori, Y. Toyama, S. Fujioka, H. Azechi, H. Fujita, H. Habara, T. Hall, Y. Izawa, T. Jitsuno, Y. Kitagawa, K. M. Krushelnick, K. L. Lancaster, K. Mima, K. Nagai, M. Nakai, H. Nishimura, T. Norimatsu, P. A. Norreys, S. Sakabe, K. A. Tanaka, A. Youssef, M. Zepf, and T. Yamanaka, "Nuclear fusion: Fast heating scalable to laser fusion ignition," *Nature*, vol. 418, pp. 933–934, Aug. 2002.

[20] V. N. Goncharov, T. C. Sangster, T. R. Boehly, S. X. Hu, I. V. Igumenshchev, F. J. Marshall, R. L. McCrory, D. D. Meyerhofer, P. B. Radha, W. Seka, S. Skupsky, C. Stoeckl, D. T. Casey, J. A. Frenje, and R. D. Petrasso, "Demonstration of the highest deuterium–tritium areal density using multiple-picket cryogenic designs on OMEGA," *Phys. Rev. Lett.*, vol. 104, no. 16, p. 165 001, Apr. 2010.

[21] T. R. Boehly, D. L. Brown, R. S. Craxton, R. L. Keck, J. P. Knauer, J. H. Kelly, T. J. Kessler, S. A. Kumpan, S. J. Loucks, S. A. Letzring, F. J. Marshall, R. L. McCrory, S. F. B. Morse, W. Seka, J. M. Soures, and C. P. Verdon, "Initial performance results of the OMEGA laser system," *Opt. Commun.*, vol. 133, no. 1–6, pp. 495–506, Jan. 1997.

[22] T. R. Boehly, D. H. Munro, P. M. Celliers, R. E. Olson, D. G. Hicks, V. N. Goncharov, G. W. Collins, H. F. Robey, S. X. Hu, J. A. Marozas, T. C. Sangster, O. L. Landen, and D. D. Meyerhofer, "Demonstration of the shock-timing technique for ignition targets on the National Ignition Facility," *Phys. Plasmas*, vol. 16, no. 5, pp. 056 302-1–056 302-9, May 2009.

[23] P. M. Celliers, D. K. Bradley, G. W. Collins, D. G. Hicks, T. R. Boehly, and W. J. Armstrong, "Line-imaging velocimeter for shock diagnostics at the OMEGA laser facility," *Rev. Sci. Instrum.*, vol. 75, no. 11, pp. 4916–4929, Nov. 2004.

[24] J. Williams, "Narrow-band analyzer (thesis or dissertation style)," Ph.D. dissertation, Dept. Elect. Eng., Harvard Univ., Cambridge, MA, 1993.

[25] J. Delettrez, R. Epstein, M. C. Richardson, P. A. Jaanimagi, and B. L. Henke, "Effect of laser illumination nonuniformity on the analysis of time-resolved X-ray measurements in UV spherical transport experiments," *Phys. Rev. A*, vol. 36, no. 8, pp. 3926–3934, Oct. 1987.

[26] P. B. Radha, C. Stoeckl, V. N. Goncharov, J. A. Delettrez, D. H. Edgell, J. A. Frenje, I. V. Igumenshchev, J. P. Knauer, J. A. Marozas, R. L. McCrory, D. D. Meyerhofer, R. D. Petrasso, S. P. Regan, T. C. Sangster, W. Seka, and S. Skupsky, "Triple-picket warm plastic–shell implosions on OMEGA," *Phys. Plasmas*, vol. 18, no. 1, pp. 012 705-1–012 705-12, Jan. 2011.

[27] F. H. Séguin, C. K. Li, J. A. Frenje, D. G. Hicks, K. M. Green, S. Kurebayashi, R. D. Petrasso, J. M. Soures, D. D. Meyerhofer, V. Y. Glebov, P. B. Radha, C. Stoeckl, S. Roberts, C. Sorce, T. C. Sangster, M. D. Cable, K. Fletcher, and S. Padalino, "Using secondary-proton spectra to study the compression and symmetry of deuterium-filled capsules at OMEGA," *Phys. Plasmas*, vol. 9, no. 6, pp. 2725–2737, Jun. 2002.

[28] J. A. Frenje, D. T. Casey, C. K. Li, F. H. Séguin, R. D. Petrasso, V. Y. Glebov, P. B. Radha, T. C. Sangster, D. D. Meyerhofer, S. P. Hatchett, S. W. Haan, C. J. Cerjan, O. L. Landen, K. A. Fletcher, and R. J. Leeper, "Probing high areal-density cryogenic deuterium–tritium implosions using downscattered neutron spectra measured by the magnetic recoil spectrometer," *Phys. Plasmas*, vol. 17, no. 5, pp. 056 311-1–056 311-9, May 2010.

[29] W. Theobald, R. Betti, C. Stoeckl, K. S. Anderson, J. A. Delettrez, V. Y. Glebov, V. N. Goncharov, F. J. Marshall, D. N. Maywar, R. L. McCrory, D. D. Meyerhofer, P. B. Radha, T. C. Sangster, W. Seka, D. Shvarts, V. A. Smalyuk, A. A. Solodov, B. Yaakobi, C. D. Zhou, J. A. Frenje, C. K. Li, F. H. Séguin, R. D. Petrasso, and L. J. Perkins, "Initial experiments on the shock-ignition inertial confinement fusion concept," *Phys. Plasmas*, vol. 15, no. 5, pp. 056 306-1–056 306-9, May 2008.

[30] W. Theobald, K. S. Anderson, R. Betti, R. S. Craxton, J. A. Delettrez, J. A. Frenje, V. Y. Glebov, O. V. Gotchev, J. H. Kelly, C. K. Li, A. J. Mackinnon, F. J. Marshall, R. L. McCrory, D. D. Meyerhofer, J. F. Myatt, P. A. Norreys, P. M. Nilson, P. K. Patel, R. D. Petrasso, P. B. Radha, C. Ren, T. C. Sangster, W. Seka, V. A. Smalyuk, A. A. Solodov, R. B. Stephens, C. Stoeckl, and B. Yaakobi, "Advanced-ignition-concept exploration on OMEGA," *Plasma Phys. Control. Fusion*, vol. 51, no. 12, p. 124 052, Dec. 2009.

[31] C. Stoeckl, J. A. Delettrez, J. H. Kelly, T. J. Kessler, B. E. Kruschwitz, S. J. Loucks, R. L. McCrory, D. D. Meyerhofer, D. N. Maywar, S. F. B. Morse, J. Myatt, A. L. Rigatti, L. J. Waxer, J. D. Zuegel, and R. B. Stephens, "High-energy petawatt project at the University of Rochester's Laboratory for Laser Energetics," *Fusion Sci. Technol.*, vol. 49, pp. 367–373, 2006.

[32] D. R. Welch, D. V. Rose, M. E. Cuneo, R. B. Campbell, and T. A. Mehlhorn, "Integrated simulation of the generation and transport of proton beams from laser-target interaction," *Phys. Plasmas*, vol. 13, no. 6, pp. 063 105-1–063 105-12, Jun. 2006.

[33] A. A. Solodov, K. S. Anderson, R. Betti, V. Gotcheva, J. Myatt, J. A. Delettrez, S. Skupsky, W. Theobald, and C. Stoeckl, "Simulations of electron transport and ignition for direct-drive fast-ignition targets," *Phys. Plasmas*, vol. 15, no. 11, pp. 112 702-1–112 702-6, Nov. 2008.

[34] W. Theobald, C. Stoeckl, V. Y. Glebov, F. J. Marshall, K. S. Anderson, R. Betti, R. S. Craxton, D. D. Meyerhofer, P. M. Nilson, T. C. Sangster, A. A. Solodov, J. A. Frenje, R. D. Petrasso, D. Hey, P. K. Patel, R. B. Stephens, R. Lauck, and P. A. Norreys, "Integrated fast-ignition experiments on OMEGA," *Bull. Amer. Phys. Soc.*, vol. 54, p. 187, 2009.

Author photographs and biographies not available at the time of publication.